Supporting Information

Fluorescence polarization-based rapid detection system for salivary biomarkers using modified DNA aptamers containing base-appended bases

Hirotaka Minagawa,[†] Akihisa Shimizu,[†] Yuka Kataoka,[‡] Masayasu Kuwahara,*[,‡] Shintaro Kato,[†] Katsunori Horii,[†] Ikuo Shiratori,*[,†] and Iwao Waga[†]
[†] NEC Solution Innovators, Ltd., 1-18-7, Shinkiba, Koto-Ku, Tokyo 136-8627, Japan
[‡] Graduate School of Integrated Basic Sciences, Nihon University, 3-25-40 Sakurajosui, Setagaya-ku, Tokyo 156-8550, Japan

***Corresponding Author**
Ikuo Shiratori
NEC Solution Innovators, Ltd.,
1-18-7, Shinkiba, Koto-Ku, Tokyo 136-8627, Japan, phone +81 3 5534 2619, fax +81 3 5534 2620
E-mail: iku-shiratori@xc.jp.nec.com

Masayasu Kuwahara
Graduate School of Integrated Basic Sciences, Nihon University,
3-25-40 Sakurajosui, Setagaya-ku, Tokyo 156-8550, Japan, phone +81 3 5317 9398
E-mail: mkuwa@chs.nihon-u.ac.jp

A tabele of content

1. SYNTHESIS OF THE MODIFIED NUCLEOSIDE TRIPHOSPHATE (dU^{gu}TP)

(1) General

NMR spectra were measured using a JNM-ECS 400 MHz NMR instrument (JEOL Ltd., Tokyo, Japan). ESI-mass spectra were recorded on an API 2000 mass spectrometer (Applied Biosystems Inc., Tokyo, Japan). Reverse-phase high-performance liquid chromatography (HPLC) analyses were performed using a HPLC system from JASCO Corporation, Tokyo, Japan. Reverse-phase medium-pressure chromatography (MPLC) was performed using an YFLC-Wprep System (Yamazen Corporation, Osaka, Japan).

(2) Materials

2,6-Dichloropurine, 2,2′-dipyridyl disulfide, *n*-tributylamine and trifluoroacetic acid (TFA) were purchased from Tokyo Chemical Industry Co., Ltd. (Tokyo, Japan). Acetonitrile and methanol for liquid chromatography LiChrosolv® were purchased from Merck Millipore (Darmstadt, Germany). Acetic acid, acetone, acetonitrile, chloroform (CH_3Cl), diethyl ether, *N*,*N*-dimethylformamide (DMF), ethylenediamine, hydrochloric acid, imidazole, 2-methoxyethanol, phosphoryl chloride, pyridine, sodium hydroxide (NaOH), triethylamine (TEA), trimethyl phosphate, and triphenylphosphine (PPh_3) were purchased from Wako Pure Chemical Industries, Ltd. (Osaka, Japan). Di-*tert*-butyl dicarbonate ($(Boc)_2O$), 1-hydroxybenzotriazole hydrate ($HOBt{\cdot}H_2O$), *N*,*N*-diisopropylethylamine (DIPEA), and benzotriazol-1-yloxy-tri(pyrrolidino)phosphonium hexafluorophosphate (PyBOP) were purchased from Watanabe Chemical Industries, Ltd. (Hiroshima, Japan). (*E*)-5-(2-Carboxyvinyl)-2′-deoxyuridine was obtained from Berry & Associates, Inc. (MI, USA).

(3) Chemical syntheses

The synthetic route of **dU^{gu}TP** is depicted in Scheme S1.

Synthesis of compound G1: A solution of di-*tert*-butyl dicarbonate (5.00 g, 22.9 mmol) in $CHCl_3$ (20 mL) was added to a solution of ethylenediamine (7.0 mL, 105 mmol) in $CHCl_3$ (120 mL) and stirred at room temperature for 24 h. The reaction mixture was filtered *in vacuo*, and the filtrate was evaporated to afford **G1** (3.57 g, 97%); ^{1}H NMR (400 MHz, $CDCl_3$) δ 3.17 (2H, q) 2.79 (2H, t) 1.44 (9H, s); ESI-MS (positive ion mode) *m*/*z*, found = 161.3, calculated for $[(M+H)^+]$ = 161.1.

Synthesis of compound G2: 2,6-Dichloropurine (1.00 g, 5.29 mmol) was dissolved in 11 mL of 2 M NaOH (aq.) and the mixture was refluxed at 90 ºC for 3 h. The reaction mixture was cooled to room temperature and filtered *in vacuo*. The residue was dissolved in water, and the pH was adjusted to 3–4 using an aqueous HCl solution (6 M). The resulting suspension was filtered *in vacuo* to afford compound **G2** (720 mg, 79%); ^{1}H NMR (400 MHz, DMSO-d_6) δ 8.29 (1H, s); ESI-MS (positive ion mode) *m*/*z*, found = 171.0, calculated for $[(M+H)^+]$ = 171.0.

Synthesis of compound G3: A solution of compound **G1** (3.28 g, 20.5 mmol) in 2-methoxyethanol (1.0 mL) was added to a solution of compound **G2** (870 mg, 5.10 mmol) in 2-methoxyethanol (5.0 mL), and the mixture was refluxed at 130 ºC for 1.5 h. The reaction mixture was cooled to room temperature, evaporated to dryness, and then recrystallized from chloroform. Compound **G3** was obtained after filtration *in vacuo* (1.12 g, 74%); ^{1}H NMR (400 MHz, CD_3OD) δ 7.34 (1H, s) 3.46 (2H, t) 3.27 (2H, t) 1.41 (9H, s); ESI-MS (positive ion mode) *m*/*z*, found = 295.3, calculated for $[(M+H)^+]$ = 295.2.

Synthesis of compound G4: Compound **G3** (500 mg, 1.70 mmol) was dissolved in TFA/MeOH (5:1, 18 mL) and the mixture was stirred at room temperature for 1 h. The reaction mixture was evaporated to dryness, and then recrystallized from diethyl ether. Compound **G4** was isolated after filtration *in vacuo* (467 mg, 89%); ^{1}H NMR (400MHz, D_2O) δ8.12 (1H, s) 3.71 (2H, t) 3.27 (2H, t); ESI-MS (positive ion mode) *m*/*z*, found = 195.1, calculated for $[(M+H)^+]$ = 195.1.

Synthesis of nucleoside dU^{gu}: To a solution of compound (*E*)-5-(2-carboxyvinyl)-2′-deoxyuridine (101 mg, 339 μmol) in dry DMF (1.0 mL), $HOBt{\cdot}H_2O$ (68.0 mg, 444 μmol), PyBOP (229 mg, 440 μmol), and DIPEA (790 μL, 4.51 mmol) were added. A solution of compound **G4** (171 mg, 412 μmol) and DIPEA (790 μL, 4.51 mmol) in dry DMF (500 μL) was then added and the resulting mixture was stirred at room temperature for 1 h. The reaction mixture was evaporated to dryness, and the residue was suspended using $CHCl_3$. Compound **dU^{gu}** was isolated after *in vacuo* filtration of the resulting suspension (147 mg, 91%); ^{1}H NMR (400MHz, DMSO-d_6) δ8.28 (1H, s) 7.62 (1H, s) 7.13 (1H, d) 7.04 (1H, d) 6.14 (1H, t) 5.26 (1H, d) 4.26 (1H, t) 4.10 (1H, q) 3.79 (1H, q) 3.67–3.56 (2H, m) 3.17 (2H, d) 2.15 (2H, q); ESI-MS (positive ion mode) *m*/*z*, found = 475.1, calculated for $[(M+H)^+]$ = 475.2.

Synthesis of compound G5: Compound **dU^{gu}** was twice co-evaporated with dry pyridine (30 mL). To a solution of compound **dU^{gu}** (101 mg, 213 μmol) in dry trimethyl phosphate (21 mL), phosphoryl chloride (400 μL, 4.29 mmol) was added and stirred in an ice bath for 2.5 h. Then, additional phosphoryl chloride (200 μL, 2.15 mmol) was added, and the reaction mixture was further stirred in an ice bath for 8.5 h. Iced water (10 mL) was added to the reaction mixture followed by 10 min stirring, and TEA (680 μL, 4.29 mmol) was further added. Stirring continued for 15 min till quench. The reaction mixture was evaporated and the residue was suspended using acetonitrile and diethyl ether. The suspension was filtered *in vacuo*, and the residue was purified by anion exchange chromatography to afford compound **G5** (23 mg, 20%); ESI-MS (negative ion mode) *m*/*z*, found = 553.0, calculated for $[(M-H)^-]$ = 553.1.

Synthesis of compound G6: Compound **G5** was three times co-evaporated with dry pyridine (5.0 mL). To a solution of compound **G5** (43.0 mg, 78.7 μmol) in dry DMF (2.0 mL), TEA (72.0 μL, 519 μmol) was added and stirring followed for 5 min. Then, imidazole (24.0 mg, 353 μmol), PPh_3 (36.0 mg, 137 μmol), and 2,2'-dipyridyl disulfide (29.0 mg, 132 μmol) were added and stirred at room temperature for 8 h. The reaction mixture was then added to a solution of anhydrous sodium perchlorate (97.0 mg, 792 μmol) in dry acetone (18 mL), dry diethyl ether (27 mL) and dry TEA (2.0 mL), and the mixture was allowed to rest at 4 ºC for 30 min. The precipitate was washed 5 times with dry diethyl ether (40 mL) to provide compound **G6** as crude material.

Synthesis of triphosphate dU^{gu}TP: The impure compound **G6** was twice co-evaporated with dry pyridine (5.0 mL). To a solution of **G6** (78.7 μmol) in dry DMF (1.0 mL), dry *n*-tributylamine (75.0 μL, 315 μmol) and dry *n*-tributylamine pyrophosphate (800 μL of a 0.5 M solution in DMF; 393 μmol) were added and stirred at room temperature for 9 h. The reaction was quenched with triethylammonium bicarbonate (1.0 M aqueous solution) (5.0 mL). The mixture was evaporated, the residue was dissolved in water, and then washed twice with diethyl ether. The aqueous layer was concentrated and purified by anion exchange chromatography and reversed-phase MPLC to yield **dU^{gu}TP** (14 mg, 25% from **G5**); ESI-MS (negative ion mode) *m/z*, found = 712.9, calculated for $[(M–H)^-]$ = 713.1.

2. SUPPLEMENTARY DATA

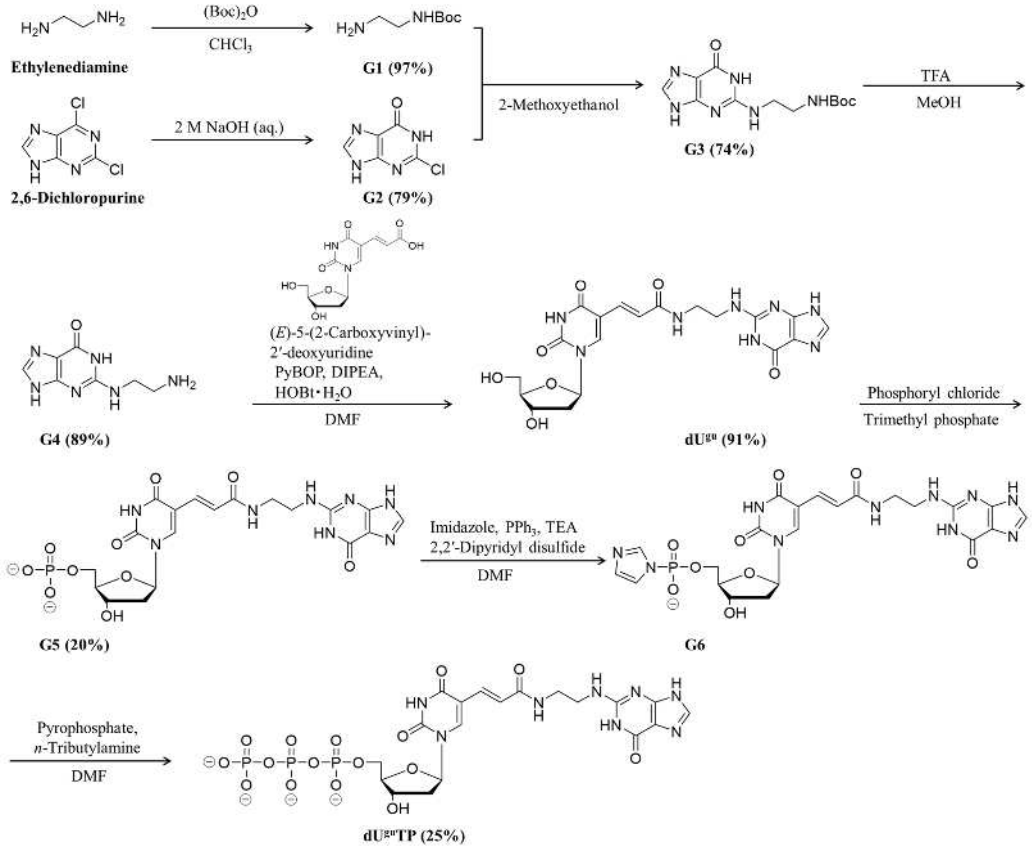

Scheme S1. Synthesis of nucleoside dU^{gu}TP.

Table S1. The 10 most common sequences derived from the U^{ad} modified ssDNA library.

Clone name	Sequence ratio[(a)]	Random region sequence[(b)]
IgA^{ad1}	7.5%	GtAtAtCAAGCAGAtGtGttCACttGGGGA
IgA^{ad2}	7.2%	AAAGAtAtGCtAAGAtAGAtAGtttGGCtt
IgA^{ad3}	7.1%	ACCtGtACtGGttAttAtGCCtGCCAACAt
IgA^{ad4}	5.4%	tttAtACGtAtGGACttAGGCtttGttAtA
IgA^{ad5}	5.1%	CtAtCtGttttAtCAAttGtAGCAAGttAt
IgA^{ad6}	4.6%	AAtCCGGCtGtAAtGCttAttAtGCCtGCG
IgA^{ad7}	4.4%	GAtGGAttAtAtGAAGtCttGGGAAGGttt
IgA^{ad8}	4.2%	AAAGttGCCGtACGCGGGtAtGCCtGGGtt
IgA^{ad9}	3.9%	AAGttCtAGtGAtAtACAGttACtAtACCt
IgA^{ad10}	3.0%	tGCttCAtACGCAGttAACCtGGttAtCAt

(a) Sequence ratio was defined as the ratio of the sequence to the total number of sequences, which was generated by next generation sequencer. (b) "t" indicates U^{ad}.

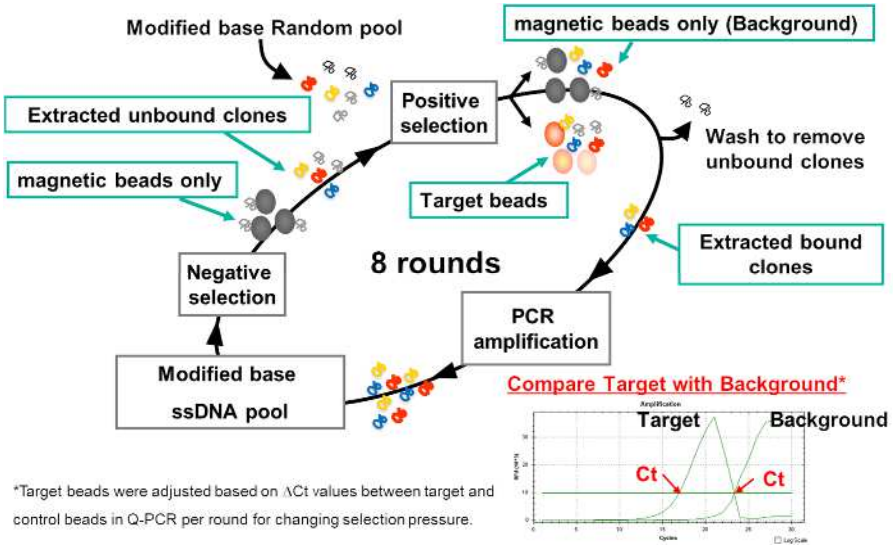

Figure S1. An illustration of the aptamer SELEX process in this report.

The quantity of target beads of positive selection step was lowered each round in response to the previous round of target/background ratio according to Gold *et. al.*[22]

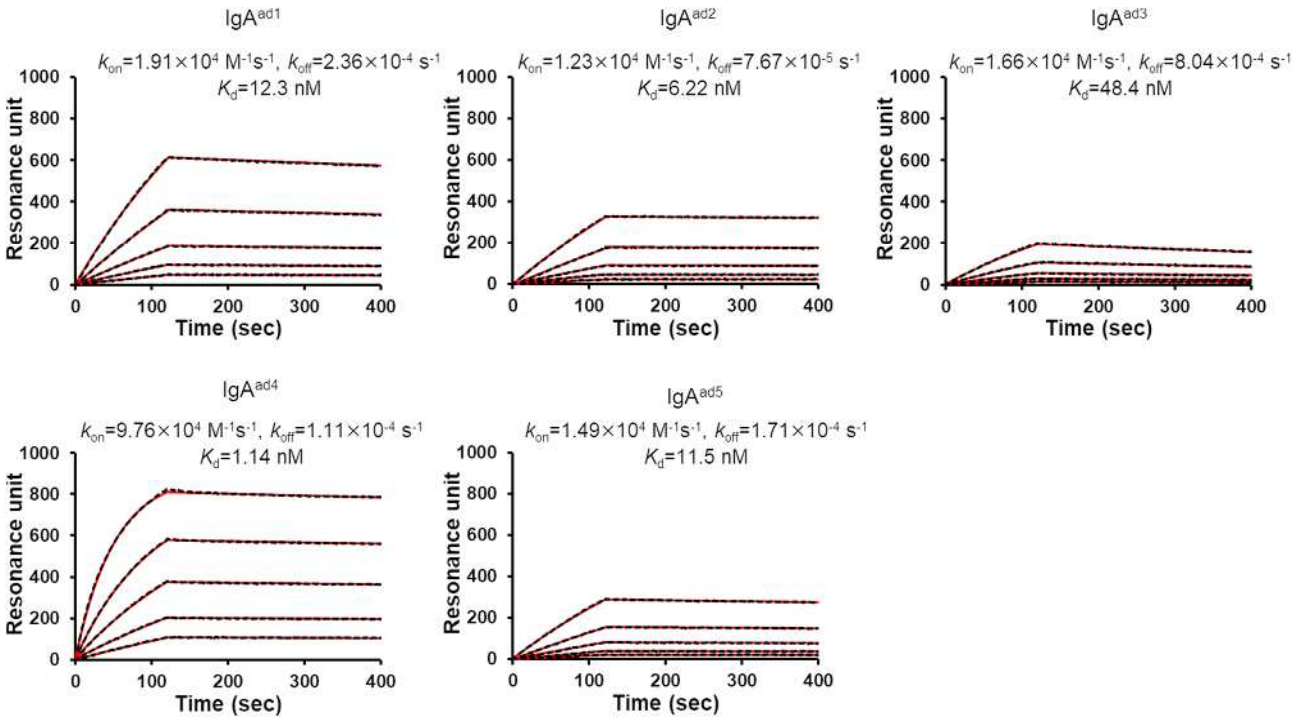

Figure S2. Representative SPR sensorgrams showing the interaction of aptamers IgA^{ad1}–IgA^{ad5} targeting SIgA. Measurements were performed with multicycle kinetics and various SIgA concentrations (12.5–200 nM) were injected over the respective aptamer-immobilizing sensor chip for 120 s at a flow rate of 50 μL/min. The black dot line represents the measured curve, and the red represents the fitting curve. The K_d values of aptamers IgA^{ad1}–IgA^{ad5} were 12.3 nM, 6.22 nM, 48.4 nM, 1.14 nM, 11.5 nM, respectively.

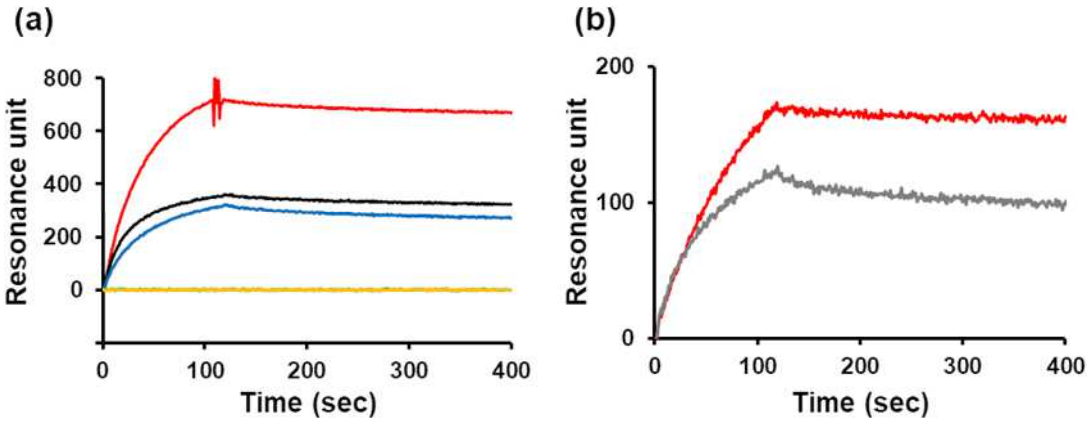

Figure S3. (a) SPR response curve of the interaction between the SIgA or several types of IgG and the aptamer IgA^{ad4}. SIgA, IgG1 kappa, IgG, or IgG-Fc (each of 400 nM) were injected over the respective aptamer-immobilizing sensor chips for 120 s at a flow rate of 50 μL/min. The red line represents the SIgA measured curve, while the black and blue lines represent the IgG1 kappa and IgG recorded curves, respectively. The green and orange lines represent the IgG-Fc1 and IgG-Fc2 measured curves, respectively. (b) SPR response curve of the interaction between the SIgA or serum IgA and the aptamer IgA^{ad4}. SIgA or serum IgA (each of 50 μg/mL) was injected over the respective aptamer-immobilizing sensor chips for 120 s at a flow rate of 50 μL/min. The red line represents the SIgA measured curve, and the gray lines represent the serum IgA measured curves, respectively.

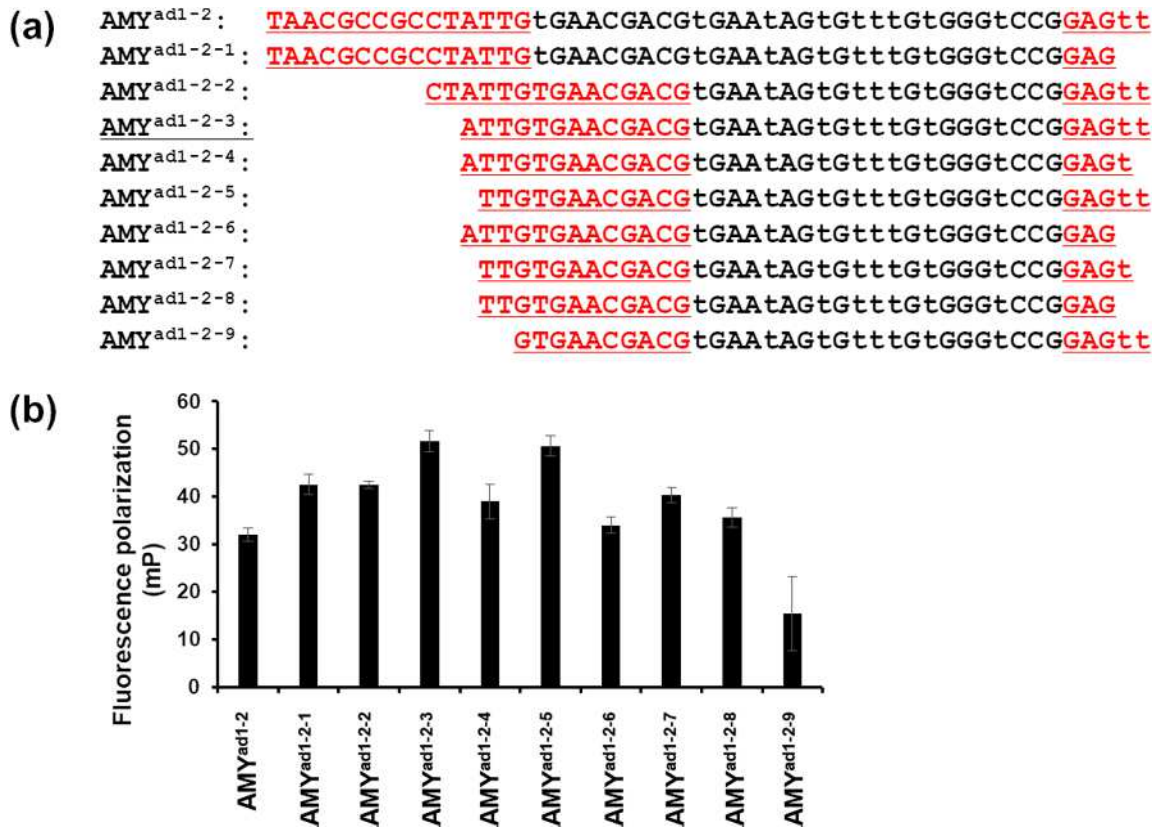

Figure S4. Sequence optimization of sAA-binding aptamers for the FP assay. (a) Sequences of the AMY^{ad1-2} truncated aptamers for the FP measurement. Sequences are aligned in the 5' to 3' direction. Underlined regions derive from the primer or primer-binding regions. (t) letters indicate the U^{ad}. The prepared clones introducing the fluorescence dye (TYE665) at the 5'-end, are shown in the table. 10 nM of the fluorescent-labeled clones were denatured at 95 ºC for 5 min, folded at 95 ºC for 5 min, and then incubated with the target samples (sAA; 10 nM and SIgA; 1 μM) in SB2 at 25 ºC for 5 min. After incubation, the samples were measured using FP spectroscopy. (b) Variation of the FP arising from the interaction between the sAA and the AMY^{ad1-2} truncated aptamers. The AMY$^{ad1-2-3}$ displayed the most FP signal changes to sAA-binding.

(a)

IgA^{gu1-3}: GCAATCTCCCTAATCtGCtGAtGtttGtAtttCAAAttAGC
IgA$^{gu1-3-1}$: GCAATCTCCCTAATCtGCtGAtGtttGtAtttCAAAtt
IgA$^{gu1-3-2}$: CAATCTCCCTAATCtGCtGAtGtttGtAtttCAAAtt
IgA$^{gu1-3-3}$: AATCTCCCTAATCtGCtGAtGtttGtAtttCAAAtt
IgA$^{gu1-3-4}$: TCTCCCTAATCtGCtGAtGtttGtAtttCAAAtt
IgA$^{gu1-3-5}$: TCCCTAATCTGCtGAtGtttGtAtttCAAAtt
IgA$^{gu1-3-6}$: CCTAATCTGCTGAtGtttGtAtttCAAAtt
IgA$^{gu1-3-7}$: TCCCTAATCTGCtGAtGtttGtAtttCAAAt

(b)

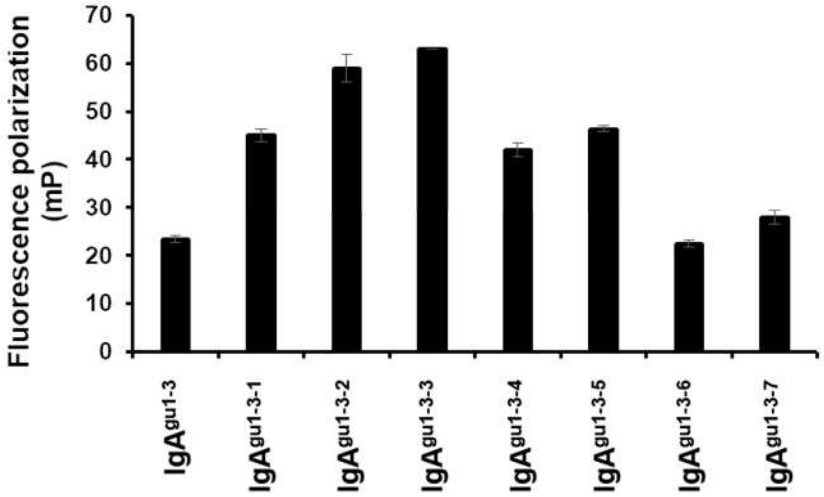

Figure S5. Sequence optimization of SIgA-binding aptamers for the FP assay. (a) Sequences of the IgA^{gu1-3} truncated aptamers for the FP measurement. Sequences are aligned in the 5' to 3' direction. Underlined regions derive from the primer or primer-binding regions. (t) letters indicate U^{gu}. The prepared clones introducing the fluorescence dye (TYE665) at the 5'-end, are shown in the table. Target samples (sAA; 10 nM and SIgA; 1 μM) were denatured at 95 ºC for 5 min, folded at 95 ºC for 5 min, and then incubated with 10 nM of the fluorescent-labeled clones in SB2 at 25 ºC for 5 min. After incubation, the samples were measured using FP spectroscopy. (b) Variation of the FP arising from the interaction between the SIgA and the IgA^{gu1-3} truncated aptamers. The IgA$^{gu1-3-3}$ displayed the most FP signal changes to SIgA-binding.

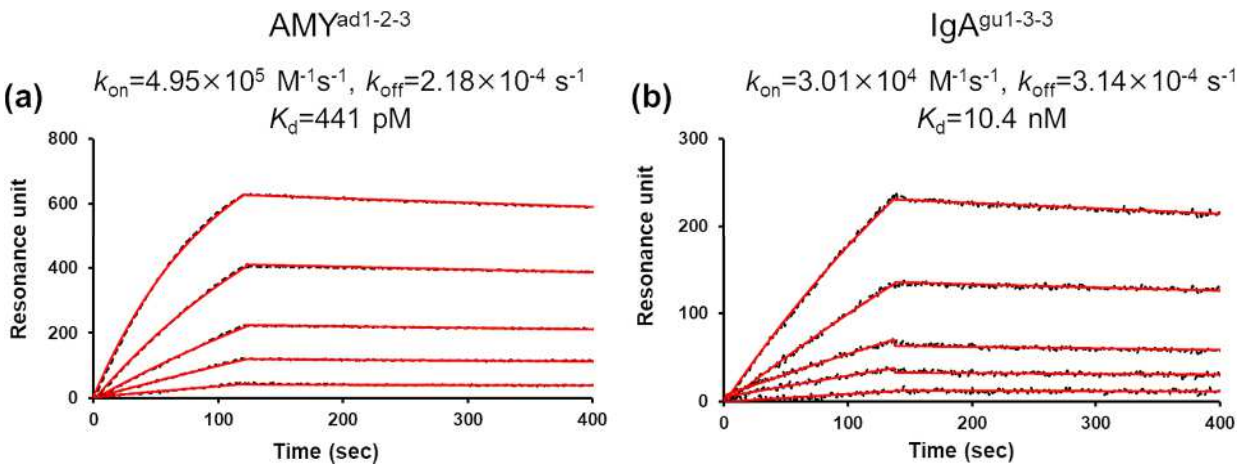

Figure S6. Representative SPR sensorgrams showing the interaction between (a) sAA and AMY$^{ad1\text{-}2\text{-}3}$ and (b) SIgA and IgA$^{gu1\text{-}3\text{-}3}$. Measurements were performed with multicycle kinetics and various concentrations of sAA (1.25–20 nM) or SIgA (6.25–100 nM) were injected over the respective aptamer-immobilizing sensor chip for 120 s at a flow rate of 50 μL/min. The black dashed line represents the measured curve and the red line represents the fitting curve.

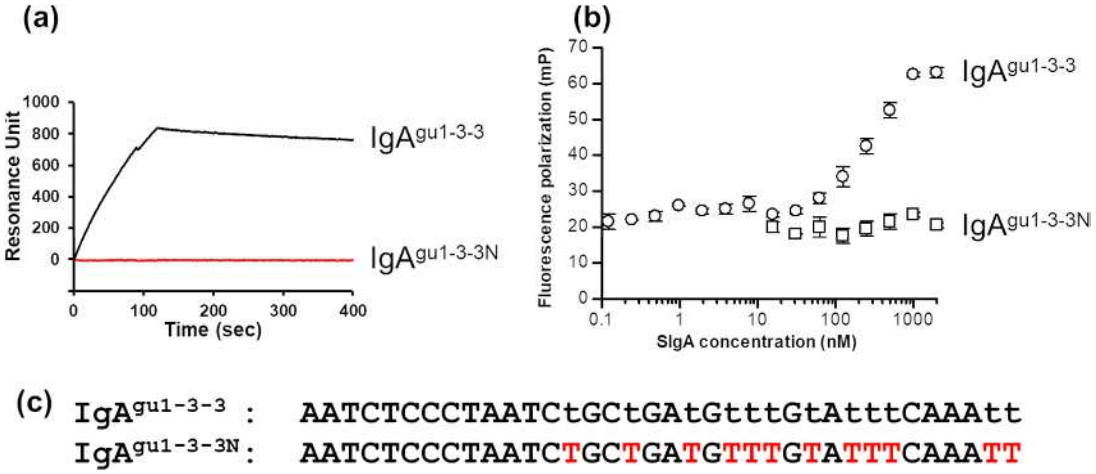

Figure S7. (a) Representative SPR sensorgrams showing the interaction between SIgA and IgA$^{gu1\text{-}3\text{-}3}$ or IgA$^{gu1\text{-}3\text{-}3N}$. Measurements were performed with concentrations of SIgA (400 nM) were injected over the respective aptamer-immobilizing sensor chip for 120 s at a flow rate of 50 μL/min. The black line represents the IgA$^{gu1\text{-}3\text{-}3}$ and the red line represents the IgA$^{gu1\text{-}3\text{-}3N}$. (b) FP calibration curves of the fluorescent-labeled IgA$^{gu1\text{-}3\text{-}3}$ and IgA$^{gu1\text{-}3\text{-}3N}$ in SB2. IgA$^{gu1\text{-}3\text{-}3}$ was incubated with 0.12–2000 nM and IgA$^{gu1\text{-}3\text{-}3N}$ was incubated with 15.6–2000 nM of the SIgA in SB2 and measured. The open circles represent the IgA$^{gu1\text{-}3\text{-}3}$ and open squares represent IgA$^{gu1\text{-}3\text{-}3N}$, respectively. (c) Sequences of the IgA$^{gu1\text{-}3\text{-}3}$ and IgA$^{gu1\text{-}3\text{-}3N}$. Sequences are aligned in the 5' to 3' direction. (t) letters indicate the U^{gu}.

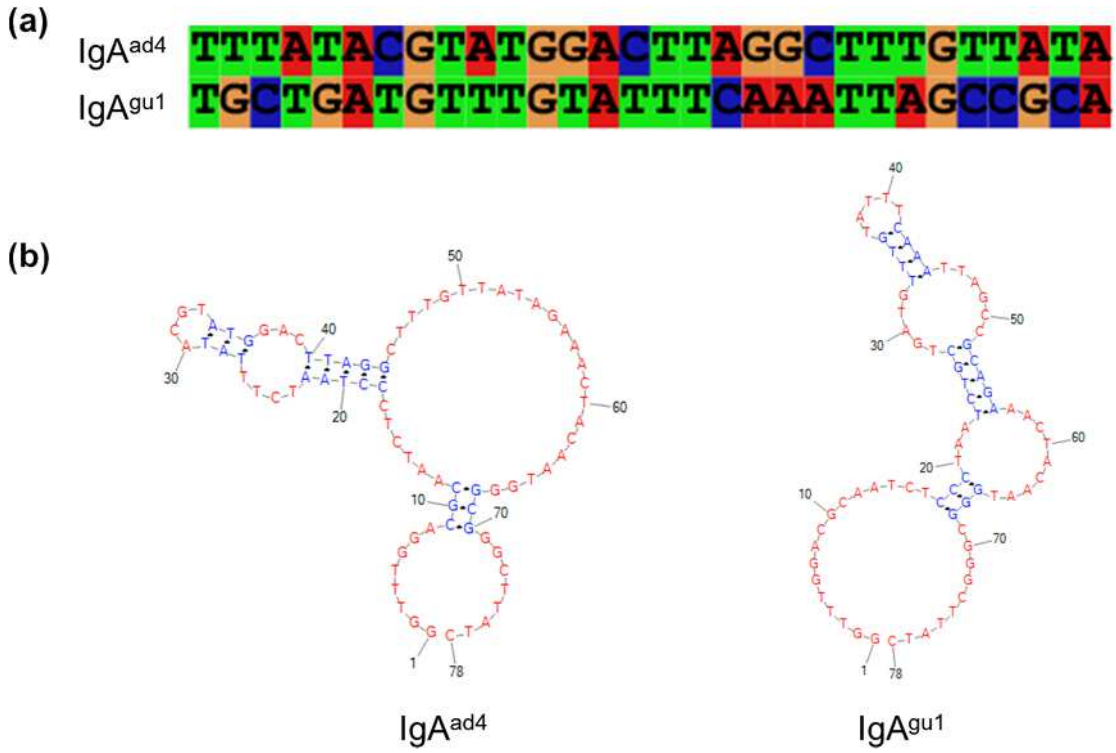

Figure S8. (a) Random region sequence comparison between IgA^{ad4} and IgA^{gu1} (b) The predicted secondary structure of IgA^{ad4} and IgA^{gu1} using VALFold program and the general DNA parameters.[34, 35]